Journal of the Iranian Chemical Society (2020) 17:1001–1011
https://doi.org/10.1007/s13738-019-01838-5

ORIGINAL PAPER

Which energetically favorable sustainable synthesis of 4-amino-8-azacoumarin ester or 4-hydroxy-3-cyano derivative based on new exact kinetic Arrhenius and DFT stimulation

Abdelfatah T. El-gendy[3] · Amr A. Youssef[2] · Sameh A. Rizk[1]

Received: 28 August 2019 / Accepted: 16 December 2019 / Published online: 21 December 2019
© Iranian Chemical Society 2019

Abstract
This article proposed the theoretical model of Arrhenius equation of differential equation with the density functional theory (DFT) to realize the structural and electronic characteristics by converting chalcone **1** to azacoumarin **4** via 2-pyridone derivatives **2**. Ultrasonic velocity, density and percentage deviation in concentration were measured by 7-aryl-5-arylidenyl-8-azacoumarin ester **4**, 3-cyano derivative **5** or 8-azachromone **6** for various temperatures. They bear conjugated moieties that are to be intended and synthesized by a concise and facile approach using ultrasound strategy. A sustainable reaction is progressed, and an efficient and eco-safe approach occurred by promoting ultrasound organic synthesis to furnish the target 8-azacoumarin **4** in a good yield. Also, Arrhenius model and DFT can be confirmed by one of the reaction ways which is the most permanent appearance. All the synthesized heterocyclic compounds were characterized via Fourier transform infrared (FTIR) spectroscopy, mass spectra, proton nuclear magnetic resonance (^{1}HNMR), carbon-13 (C13) nuclear magnetic resonance (^{13}CNMR) and elemental analyses.

Keywords Arrhenius model · DFT · Green synthesis · Synthesized curcumin · 8-Azacoumarin

Introduction

Dynamic combinatorial chemistry (DCC) describes the generation of dynamic chalcone-pyrid-2-one and azacoumarin compounds by reversibly reacting with building blocks. These compound libraries, which are under thermodynamic control, remain adaptive by continuous interconversion coumarin–chromone products, which are explained by Arrhenius equation model. Therefore, the addition of azacoumarin target alters their equilibrium composition by binding, thereby stabilizing and ultimately amplifying specific library constituents [1–3]. Arrhenius equation is a famous differential equation of first order to describe the thermal chemical reaction during the non-isothermal process [4]. Target-directed DCC, thermogravimetric analysis (TGA), differential thermogravimetry (DTG), equilibrium temperature of chemical reaction T_{Eq} and G_{SB} exhibit a self-screening ability and a valuable tool for drug discovery, leading to the amplification of those members of the library with the highest affinity for the azacoumarin target, as depicted for curcumin precursors in Figs. 1, 2, 3, 4, 5, 6, 7, 8 and 9 (see more in appendix file). On the other hand, the quantum mechanical program was used for the molecular parameters such as chalcone, pyridine and azacoumarin compounds for the most potent bio-compounds [5–9]. Moreover, the minimal energy of geometrical configuration for the most potent antioxidant curcumin and azacoumarin compounds is obtained [10]. The density function theory (DFT)-based quantum calculations can give insights into the structural and electronic characteristics of organic molecules [11]. Herein, the parameters are obtained from the DFT study of 8-azacoumarin derivatives, which are performed by the energies of Frontier molecular orbitals, e.g., highest

Electronic supplementary material The online version of this article (https://doi.org/10.1007/s13738-019-01838-5) contains supplementary material, which is available to authorized users.

✉ Abdelfatah T. El-gendy
elgendy25@hotmail.com

[1] Organic Chemistry, Chemistry Department, Science Faculty, Ain-Shams University, Cairo, Egypt

[2] Department of Basics Science (Applied Mathematics), High Institute for Engineering and Technology, El-Beheira, Egypt

[3] Physics Department, Science Department, Ain-Shams University, Cairo 11566, Egypt

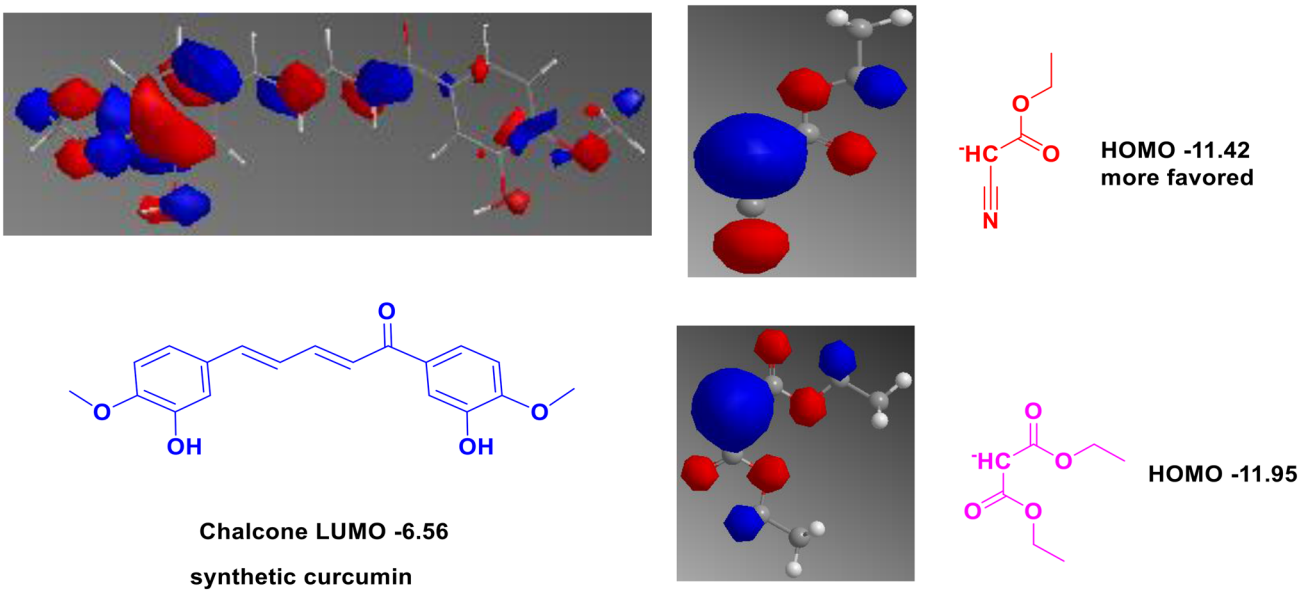

Fig. 1 Optimization via computational chemical calculation outlines LUMO of curcumin which matches with both HOMO ethyl cyanoacetate and diethyl malonate

occupied molecular orbital (HOMO) energy (E_{HOMO}) is a parameter of a direct relation to the ionization potential and its value expresses the susceptibility of organic molecule toward attacks by electrophiles, whereas lowest unoccupied molecular orbital (LUMO) energy (E_{LUMO}) refers to the electron affinity and its value expresses the vulnerability of the molecule toward a nucleophilic attack [12]. HOMOs are distributed over the aryl and arylidene units, while LUMOs are focused on the azacoumarin moiety. In the chemical kinetic model, curcumin is thermally dissolved in the non-isothermal process to produce new azacoumarin compounds using an analytical solution for this equation in order to have a new study of how 8-azacoumarin derivatives are chemically converted [13–15].

In this study, we have been synthesizing the 8-azacoumarin derivatives **4** and **5** via chalcone **1** or 2-pyridone derivatives **2** and **3** [16–18] and will be recalled that based on the values derived from the mathematical Arrhenius model and the quantitative program (DFT) to study the molecules that the first interaction will be likely to occur and appear more than the second in terms of results that the degree of heat temperature (TGA), which refers to the separation between the transition from another phase is greater than the temperature of the transition less From the middle of the reaction, allowing for the possibility of a lower probability of reversion in the reaction and the degree of equilibrium and strike rate closer than the second interaction.

Materials and methods

Mathematical model of kinetics estimation

Arrhenius equation is expressed in terms of the residual mass fraction of degradable material $1-\chi$, in order to produce new materials of mass conversion fraction χ, by the thermal decomposition as follows:

$$\frac{d\chi}{dt} = k(T)(1-\chi)^n \tag{1}$$

where $d\chi/dt$ is a time rate of mass conversion fraction χ, to describe the activity of the thermal chemical reaction in the non-isothermal process, n is an order of the chemical reaction and $k(T)$ is a constant rate, which was introduced by Arrhenius as follows:

$$k(T) = A\ \mathrm{Exp}(-E/RT) \tag{2}$$

where A is a pre-exponential factor, E is an activation energy, T is a temperature and R is a constant gas. The mass conversion fraction χ of the thermally dissolved material is given by:

$$\chi = \frac{m_0 - m(t)}{m_0 - m_f} \tag{3}$$

where $m_0, m(t)$ and m_f are the initial mass, mass at a time t and final mass of a degradable material, respectively. According to experiments of thermal chemical reactions, the heating rate is taken as constant $\beta = dT/dt$. Hence, the

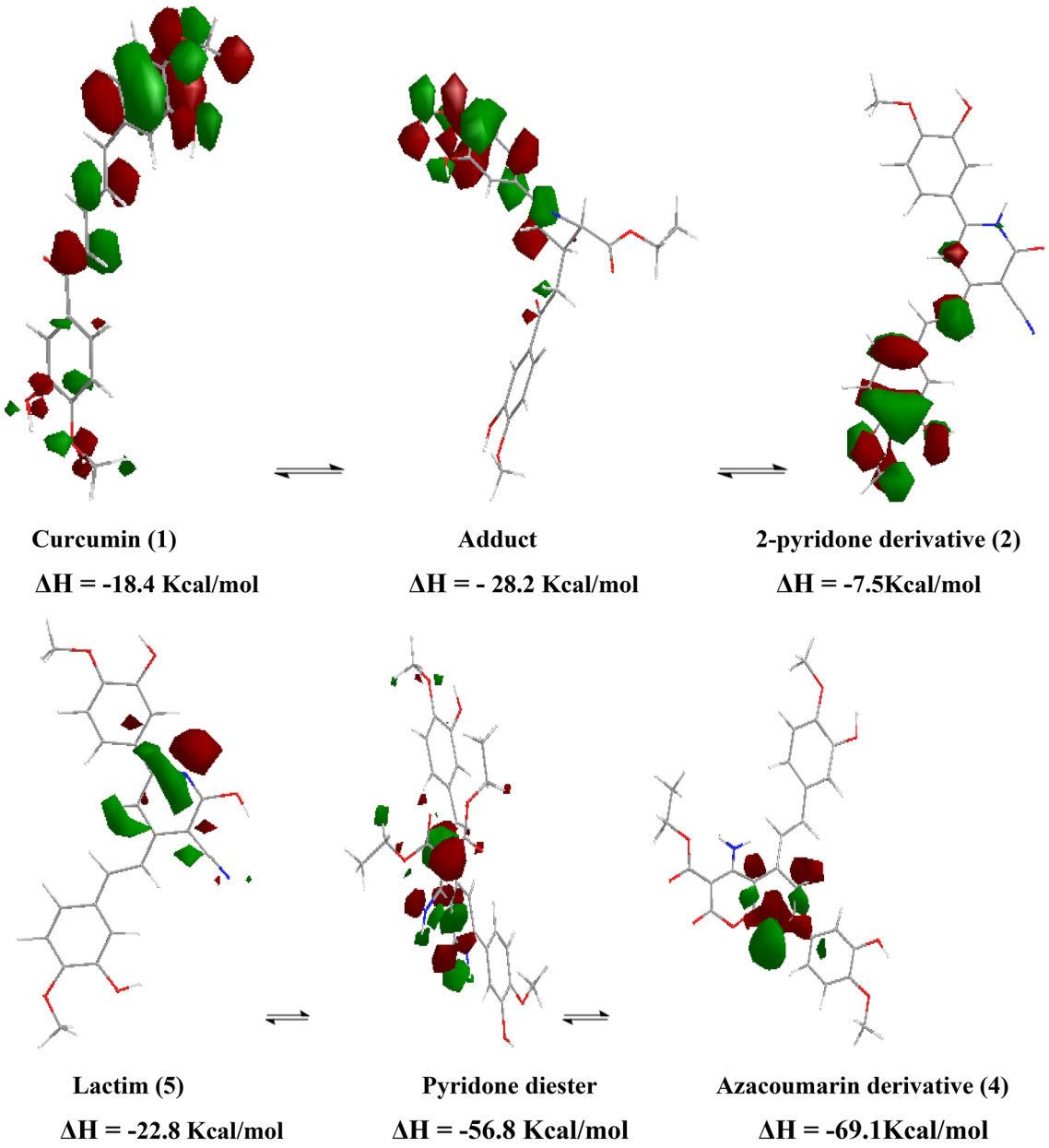

Fig. 2 Optimization via computational chemical calculation converted chalcone 1 to azacoumarin 4 via 2-pyridone derivatives 2

constant heating rate in the kinetic analysis of data for the thermal decomposition is described by:

$$\beta = \frac{T_f - T_0}{\tau_i} \tag{4}$$

where T_0 and T_f are the initial and final temperatures, and τ_i is a time of the thermal decomposition from the initial to final temperatures. Therefore, the rate of mass conversion fraction with respect to temperature is expressed as:

$$\frac{\mathrm{d}\chi}{\mathrm{d}T} = \frac{A}{\beta} e^{-(E/R)/T}(1-\chi)^n, \tag{5}$$

Finally, for $n = 1$, Eq. (6) is solved by the method of separation variables and is rewritten as:

$$\int_0^{\chi} \frac{\mathrm{d}\chi}{1-\chi} = \frac{A}{\beta} \int_{T_0}^{T} \mathrm{e}^{-(E/R)/T} \mathrm{d}T \tag{6}$$

The temperature integral in the right-hand side of Eq. (7) is evaluated analytically in terms of the generalized hypergeometric function ${}_2F_2$ and the natural logarithm. Hence, the exact analytical solution is described by:

$$1 - \chi = \exp\left[H(T)\right] \tag{7}$$

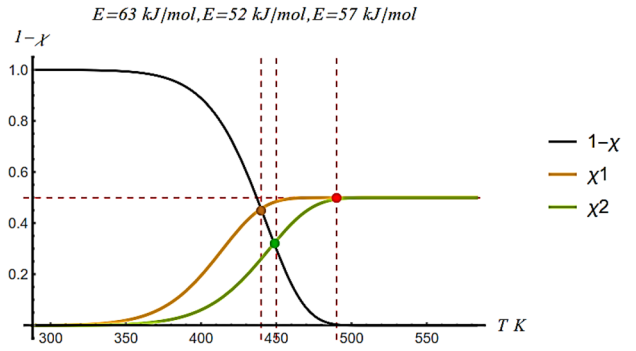

Fig. 3 TGA capture relation between residual mass and its products of minimum full thermal mass decomposing temperature of [brown point) (green point). The amount of absorb energy is little high

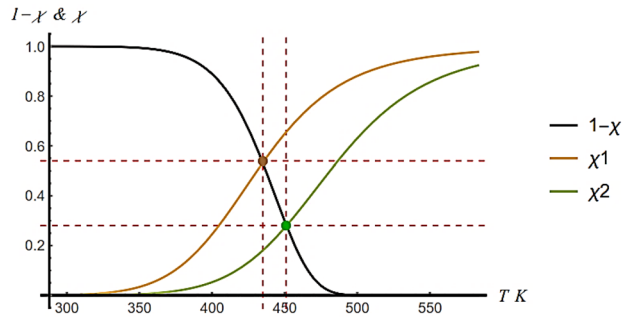

Fig. 4 TGA intersects with equilibrium conversion between pyrid-2-one **2** (brown point) and azacoumarin **4** (green point) at 435 °K and 451 °K

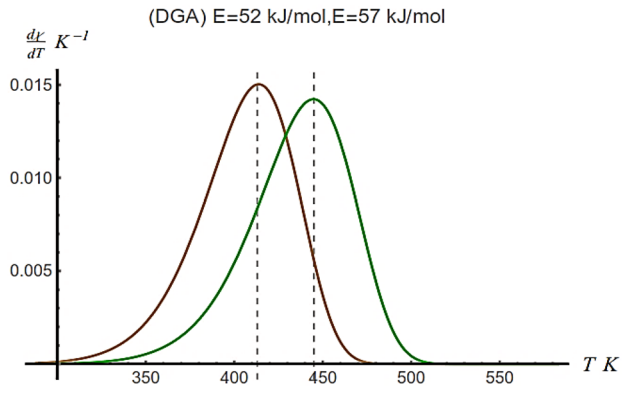

Fig. 5 DTG of exact full half thermal decompose of residual mass of azacoumarin products at 410 °K and 445 °K

where $1-\chi$ is the residual mass fraction and $H(T)$ is dimensionless function because all terms are dimensionless, and it is given by [19]:

$$H(T)=\frac{T_0-T}{\alpha}+\frac{\delta}{\alpha}\ln\left(\frac{T}{T_0}\right)+\frac{\delta^2}{2\alpha T_2}F_2\left(1,1;3,2;-\frac{\delta}{T}\right)-\frac{\delta^2}{2\alpha T_{0\,2}}F_2\left(1,1;3,2;-\frac{\delta}{T_0}\right) \tag{8}$$

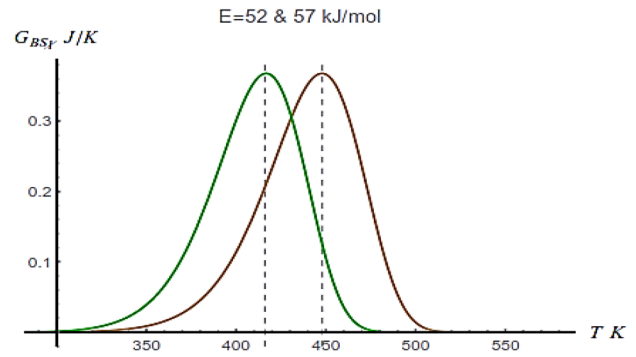

Fig. 6 $G_{\mathrm{SB}\chi}$ of pyrid-2-one **2** and azacoumarin **4** which capture the exact temperature (416 °K and 450 °K) of phase transition to new product at the lowest disorder of the chemical reaction

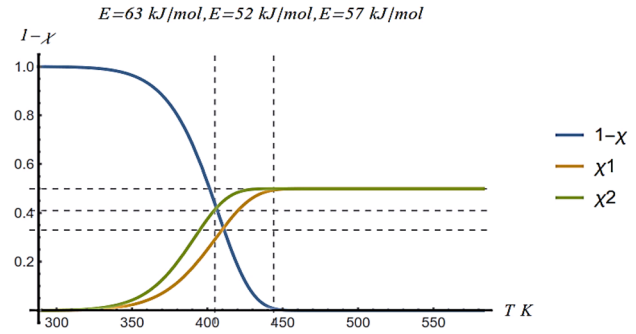

Fig. 7 TGA capture relation between residual mass of curcumin **1** and its products of pyrid-2-one **2** and azacoumarin **4** at full thermal mass decomposing temperature of [brown point)/(green point)], respectively

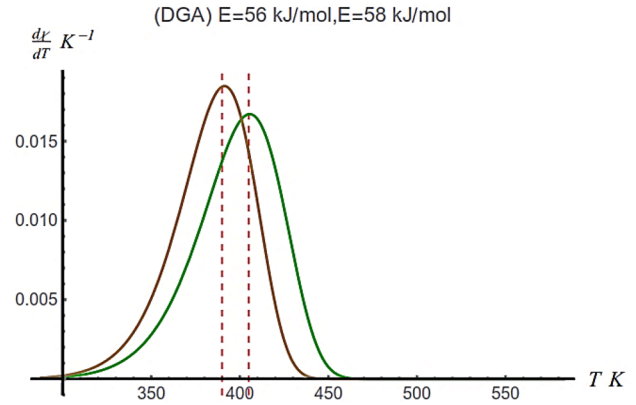

Fig. 8 DTG of exact full half thermal decompose of residual mass of curcumin **1** and its products at 392 °K and 407 °K

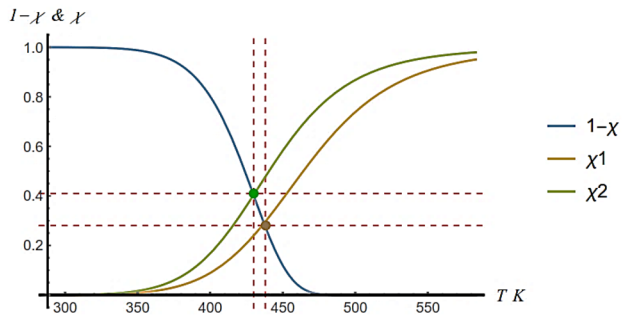

Fig. 9 TGA intersects with equilibrium conversion [brown point)/(green point)] at 430 °K and 438 °K

where $\alpha = \beta/A$ and $\delta = E/R$, R is the gas constant. Thus, for n = 1, the exact analytical solution is obtained for Arrhenius equation at a constant heating rate in non-isothermal kinetics. The most common methodology during the thermal composition adopted by various researchers is thermogravimetric analysis (TGA). In our study, the exact analytical solution (7,8) is used to get more reliable conclusions of our chemical reactions. Moreover, the differential thermogravimetry (DTG) (5) is calculated analytically by Eqs. (7, 8), and it is expressed as:

$$\frac{\mathrm{d}\chi}{\mathrm{d}T} = \alpha \exp\left[H(T) - \frac{\delta}{T}\right] \tag{9}$$

The thermal equilibrium conversion of the constant rate of Arrhenius equation is a translation step to get new solid materials, which may be obtained by [20]:

$$\in = \frac{k_e(T)}{1 + k_e(T)} \tag{10}$$

where

$$k_e(T) = k_m \exp\left[\frac{\Delta H}{R}\left(\frac{1}{T_m} - \frac{1}{T}\right)\right] \tag{11}$$

where k_m is the equilibrium constant at the temperature T_m (K), and ΔH is the heat of reaction (J/mol). A Boltzmann–Gibbs entropy is obtained from the statistical mechanics in order to obtain the accurate results about the thermal equilibrium conversion for the thermal chemical reaction. The thermal equilibrium conversion is investigated by a Boltzmann–Gibbs entropy for the residual mass fraction, which is determined by solving the Arrhenius equation in the exact analytical form. The Gibbs–Boltzmann entropy of a residual mass fraction is accomplished as follows [21, 22]:

$$S_{GB\chi} = -K_B(1-\chi)\ln((1-\chi)) \tag{12}$$

Thus, the aim of a Boltzmann–Gibbs entropy is achieved by the exact temperature of the fluctuated phase to get a new intermediate material with very low disorder of state.

Experimental chemistry

Melting points were measured in open glass capillaries. The FTIR spectra (υ_{max} in cm^{-1}) were chronicled on FTIR Spectrophotometer Shimadzu-8400S with KBr pellets (New York, USA). ^{1}H-NMR spectra were recognized on 300 MHz spectrophotometer (Rheinstetten, Germany) using $\delta = 2.50$ and 3.50 for DMSO-d_6 as solvents and TMS as an internal standard. ^{13}C-NMR spectra at 100-MHz spectrometer (Rheinstetten, Germany) is referenced to solvent signals $\delta = 39.50$ ppm for DMSO-d_6. The mass spectra were noted on Shimadzu GCMS-QP-1000 EX mass spectrometer (Kyoto, Japan) at 70 eV for electron ionization. Elementar Vario automatic CHN analyzer (Lucknow, India) was used for elemental analyses and was recorded at central armed force. Sonication has a frequency of 100 kHz and operates at maximum power of 150 W in a Toshcon model SW 4 cleaner which was achieved by the synthesized azacoumarin. Purification of compounds was checked by TLC using silica gel (120–60) mesh) as eluate, UV light. All common reagents and solvents were without further purification from commercial suppliers. Chalcone (curcumin **1**) and pyridine-2-one (**2** and **3**) were prepared by the method described in the literature [16–18].

General procedure for the synthesis of azacoumarin derivatives (4), pyrano-2,7-naphthyridine (N-Michael)

Chalcone **1** (0.05 mol), or pyridine-2-one **2** and **3**, and ethyl cyanoacetate or diethyl malonate (0.05 mol) in the presence of ammonium acetate (0.1 mol) were ground together in a mortar. Then, this mixture was transferred into a 250-mL round bottom flask with the addition of ethanol (15 mL). The reaction mixture was located in the maximum energy area in an ultrasonic cleaning bath. The bath temperature was controlled by the addition or removal of water at 70 °C. The progress of the reaction was monitored by TLC using C_6H_6: EtOAc 95:5. Sonication was continued until starting reactants disappeared as designated by TLC. A yellow solid product was yielded within 30–35 min of irradiation. After the reaction completion, the product was decanted into crushed ice with constant stirring to obtain a yellow solid mass, which was dried and recrystallized from ethanol.

Target-directed dynamic combinatorial chemistry (TGA, DTG and G_{SB})

Since the outcomes of TGA and DTG experiments are influenced by the ratio of scaffolds to fragments of synthesized

curcumin and pyrid-2-one and target azacoumarin constituents [23, 24], we studied this issue in more detail by employing different amounts of building blocks, while keeping the azacoumarin product concentration constant. Dynamic libraries were generated with varying concentrations of curcumin scaffold **1** (600 μM, 400 μM and 200 μM) together with ethyl cyanoacetate and diethylmalonate fragments each at 100 μM. All libraries were equilibrated in the presence and absence of 100 μM (restrained in Arrhenius parameters). In this experimental design, the amount of chalcone scaffold **1** is determining the maximum attainable curcumin concentration. Assuming full conversion of the azacoumarins **4**, **5** and azachromone **6** facilitated by the addition of excess diethylmalonate/ethyl cyanoacetate, concentration ratios of 4:1, 3:1 and 2:1, respectively. High % yield of Azacoumarin **4** and N-Michael product should be reached with a 1:1 ratio, accurate detection and was not possible formed azacoumarin **5** and azachromone **6** due to a sufficient amount of the highly reactive ethyl cyanoacetate, i.e. high % of the 3-cyano pyrid-2-one **2** and unsatisfactory attendance of the pyrid-2-one ester **3** and unsatisfactory attendance of the pyrid-2-one ester **3** (Scheme 2). The libraries were analyzed by UV-HPLC, detecting optical density at 310 nm. Conveniently, only azacoumarin **4** absorbs UV light at this particular wavelength, but not other library constituents such as curcumin, unreacted ethyl cyanoacetate at the ratio of 1:1. Peaks in the resulting chromatograms were assigned using reference samples. At the concentration ratio 2:1, both azacoumarin (**4**) and azachromone (**6**) gave overlapping signals, which could not be resolved; we treated these signals as both constituents contain % yield of 38 and 23.

Results and discussion

Chemistry

An accelerated concern about environment and safety has attracted global efforts to develop green eco-friendly procedures. Therefore, ultrasound promoted synthesis in aqueous media (cheap, safe and environmentally benign solvent) [25] and solvent-free synthesis [26] had emerged and are increasingly used in organic synthesis due to more environmentally tolerant, easily controlled, higher yield, shorter reaction time and milder condition. More convenient and rapid synthetic procedures that are energy efficient became highly desirable such as grindstone and one-pot multi-component reactions (MCRs) [27]. This kind of green chemistry is widely used nowadays and became significant in combinatorial chemistry due to its process simplicity, mild conditions, atomic economy and extension of the scope of substrates. 8-Azacoumarin is coumarin isostere have pyridyl group in its place of phenyl leads to increase the hydrophilicity and improve metabolic stability as antioxidant substance. Therefore, azacoumarins have emerged as a plausible class of biological candidates, but they have not received enough attention [28]. Only few 8-azacoumarins, however, were prepared before due to the inherent poor nucleophilicity of pyridines, which means that this method is only suitable for those electron-rich pyridines, resulting in a limited number of accessible targets. Recently, a new method for the synthesis of 8-azacoumarins that would greatly extend the substrate scope has been reported via ultrasonic methods [16–18]. In the present work, we reported that the one-pot reaction of chalcone **1**, ethyl cyanoacetate and diethyl malonate in the presence of ammonium acetate was submitted to react in a multi-component reaction (MCR), or the pyridine-2-one derivatives **2** and **3** were reacted with 2-substituted ethyl acetate via two-component reactions in ultrasonic reaction conditions to afford crude yellow solid product of the 8-azacoumarin derivatives **4** and **5**, respectively, for 30–35 min and the N-adduct via 2-pyridone **2** [16, 17] (Scheme 1). The reaction takes place through group-assisted purification (GAP) [18], in which we describe a process where special functional groups are devoted to reaction substrates and facilitating purification of crude products by avoiding traditional purification methods such as chromatography or recrystallization. Both the above-supposed techniques provided products in good-to-excellent yields with simple and mild reaction conditions. Applying the Arrhenius equation in the product synthesis can greatly reduce the generation of second route of the competitive pyridine ester 3, and the formation of pure 3-cyano pyridine-2-one intermediate **2** followed by ring closure using ammonium acetate to afford high yield of the azacoumarin target **4** in addition to N-Michael adduct. From Table 1, we can conclude from the % yield of reaction subsequent treating of curcumin **1** with ethyl cyanoacetate and diethyl malonate afforded major product of azacoumarin **4**, minor % yield of Azacoumarin **5** and surprising, isolated the Azachromone product **6** in appropriate yield. The HOMO energy of the ethyl cyanoacetate anion at − 11.4 eV inverses its reactivity toward the curcumin **1** much more than diethyl malonate precursor, which at 11.7 eV is outlined in Fig. 1. Moreover, increase in the TGA of MCRs of the curcumin, ethyl cyanoacetate and diethylmalonate revealed the thermodynamically control of the 3-cyano pyrid-2-one **2** (later we see more). Optimization structures of the reactant curcumin **1** and 8-azacoumarin product **4** via DFT outlined the reaction sequence through 3-cyano pyrid-2-one **2** (Fig. 2).

However, DFT based on the Arrhenius model designated 3-cyano-2-pyridone derivatives **2** that have lower $\Delta H = -7$ kcal/mol isomerized to the reactive lactim intermediate and proceeded with ethyl diethylmalonate under three-component reactions which afforded the energetically favorable azacoumarin **4** as a major product $\Delta H = -76.64.1$ kcal/mol (Figs. 1 and 2). The authors

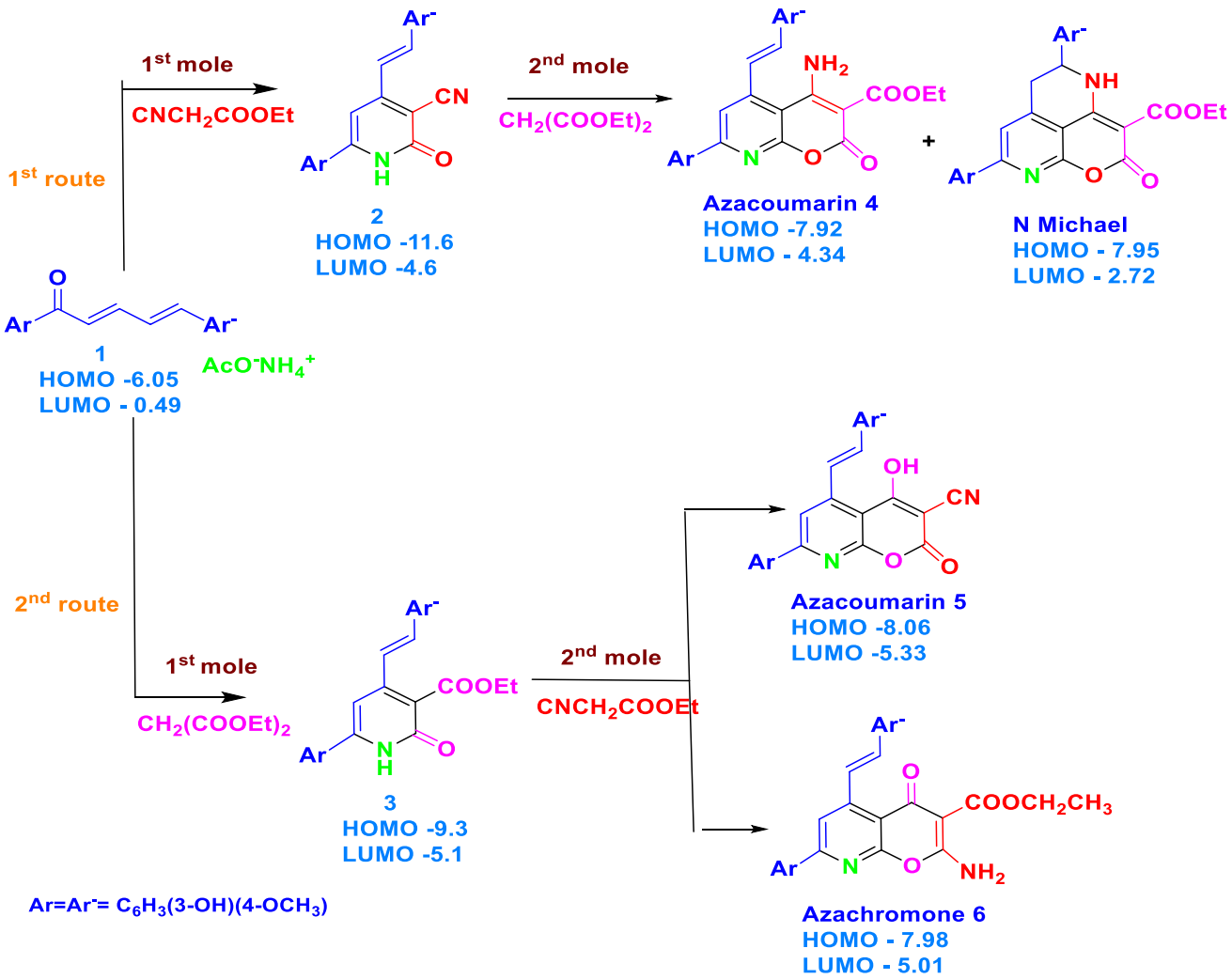

Scheme 1 It outlines which ultrasonic reaction is more permanent for isomerization?

Table 1 Quantum chemical parameters calculated for the studied compounds. *I*, ionization potential; *A*, electron affinity; *X*, electronegativity; *η*, hardness; *σ*, softness; ΔH, enthalpy; *μ*, dipole moment; *Amolec*, surface area

Compound	E_{HOMO} (eV)	E_{LUMO} (eV)	ΔE (eV)	I (eV)	A (eV)	χ (eV)	η (eV)	σ (eV^{-1})	ΔH ($KJmol^{-1}$)	μ (Debye)	A_{molec} (nm^2)
4	−7.92	−4.43	3.49	7.09	4.38	5.74	1.35	0.714	320.66	8.790	597.443
5	−8.06	−5.33	2.73	8.18	5.13	6.66	1.53	0.654	222.17	11.558	542.608
6	−7.98	−5.01	2.97	7.66	2.66	5.17	2.50	0.403	317.32	12.139	590.401
N-Michael	−7.95	−2.72	5.23	8.13	2.63	5.39	5.45	0.182	251.74	9.395	519.866

confirmed the target azacoumarin product **4** via treatment of the isolated 3-cyanopyridine-2-one **2** with diethylmalonate. Structures of all the synthesized compounds were established on the basis of elemental and spectral analyses (IR, NMR and MS). As an evidence in the IR spectra, the characteristic peaks at 1749–1737 cm^{-1} corresponded to stretching frequency of carbonyl (νC=O) lactone and ester groups of all 8-azacoumarin (**4**) and disappeared (νC=O) at 1667–1660 of curcumin **1**. Moreover, the appearance of the stretching vibration of NH_2 as broadband is in the region of 3440–3370. The ^{1}H-NMR spectra of novel 8-azacoumarin derivative **4** revealed characteristic singlet peaks δ=10.11 and 9.82 ppm region corresponding to OH and NH_2 groups, respectively. On

the other hand, ^{1}H-NMR spectrum of N-Michael adduct revealed characteristic singlet peaks at δ=6.47–6.82 ppm region corresponding to NH moieties. In addition, a multiplet peak at δ = 6.79–8.01 ppm region corresponding to the protons of aryl and 1H of pyridyl rings emerged from synthesized compounds, which clearly ascertained their corresponding molecular structures.

DFT-based characterization

The quantum mechanical program was used for the molecular parameters for the azacoumarins **4**, **5**, azachromone **6** and N-Michael adduct and their fully optimized minimum energy geometrical configuration, which are listed in Table 1. To obtain these parameters, the molecule must be subjected first to geometry optimization, and then, these parameters are calculated. The HOMO and LUMO distributions are displayed in supplementary file. Evidently, HOMOs are distributed over the aryl and arylidene units, while LUMOs are focused on the azacoumarin moiety. The azacoumarin **4** has E_{HOMO} − 7.92, E_{LUMO} − 4.43, so ΔE = 3.49 eV = 80.20 kcal/mol and ΔH = − 320.69 kJ/mol, the azacoumarin **5** has E_{HOMO} − 8.06, E_{LUMO} − 5.39, so ΔE = 2.67 eV = 61.36 kcal/mol and ΔH = − 222.58 kJ/mol, the azachromone **6** has E_{HOMO} − 7.98, E_{LUMO} − 5.01, so ΔE = 2.97 eV = 68.25 kcal/mol and ΔH = − 317.32 kJ/mol and the N-Michael product has E_{HOMO} − 7.95, E_{LUMO} − 2.72, so ΔE = 5.23 eV = 120.19 kcal/mol and ΔH = − 251.74 kJ/mol. The former computational results are in good agreement with the experimental % yield of the products in which azacoumarin **4** has 38%, azacoumarin **5** has 11%, azachromone **6** has 23% and N-Michael adduct has 16%, respectively. However, the azacoumarin **4** has coincidental favored route 1 that are outweighed enough to increase the % yield of azacoumarin **4** than the other isolated products; nevertheless, the presence of identical functional groups in azacoumarin **4** and azachromone **6** has approximately ΔH equal (see more in Table 5 and supplementary file).

Therefore, quantum chemical calculation via DFT designates the 8-azacoumarin moieties which have more active centers for electron transfer through electron donation or acceptor. The obtained E_{HOMO}, E_{LUMO}, hardness (η), softness (σ) and enthalpy (ΔH) of the synthesized compounds are listed in Table 1. Consequently, and based on the results of converted chalcone **1** to azacoumarins **4, 5** and azachromone **6** via 2-pyridone derivatives **2** and **3**, the model of exact solution of Arrhenius equation and the quantum mechanical program DFT gives a good agreement.

Results using our analytical model of reaction

In this study, we will introduce our exact solving model of Arrhenius equation. Several important kinetic temperatures are achieved such as thermal gravimetric analysis (TGA), differential thermal gravitometer (DGA), maximum of equilibrium temperature conversion (T_{Eq}) and Gibbs entropy (G_{SB}) of the residual mass. Every physical parameter is indicated to a significant chemical kinetic reaction. Equation 7 can measure the TGA of relation of the residual mass with temperature from the graph; we could measure the full half transform of non-isothermal process at constant temperature. Equation 9 can determine the DGA of the phase transfer of changing residual mass, which relates to more stable chemical reaction, which is one of the important outcomes of comparison between the temperature of TGA and DGA. If the temperature of TGA is greater than DGA, the reaction is more reverse in its chemical reaction process and vice versa. On the other hand, the physical meaning of TEC is the temperature of equilibrium in which the reaction reaches the most stable state. Moreover, the temperature of Gibbs entropy is the temperature of less disorder of the chemical process. If the temperature of TEC and Gibbs entropy is approximately equal, it confirms a more stable low disorder reaction and final transfer of chemical reaction. By calculating the normalized changes of relative peak area (RPA) between curcumin (**1**) and azacoumarin (**4**), the influence of TGA, DTG and G_{SB} could be assessed. Surprisingly, the library composition observed post-equilibration was influenced by the curcumin and azacoumarin TGA, DTG and G_{SB} ratio (4:1, 3:1 and 2:1), where differences between components became more enhanced with greater relative

Table 2 The result of residual mass TGA, DGA, temperatures of conversion equilibrium point and its confirmation of finding Gibbs entropy using our exact model of Arrhenius equation the cyano pyrid-2-one **2**, azacoumarin **4** and N-Michael adduct

Compound	Maximum temperature of TGA	Maximum temperature of DTG	Maximum temperature of conversion equation	Gibbs entropy (J/K)	Time duration of full chemical process
2	435	442	–	446	148
$(1-\chi_i)^2$	0.5	0.41	–	0.35	
4	–	410	420	415	
N-Michael	–	440	446	445	

Table 3 Activation energy and entropy of Arrhenius equation the cyano pyrid-2-one **2**, azacoumarin **4** and N-Michael adduct

Compound	Activation energy (KJ)	Exponential factor A $*10^6$	Entropy (J/mol)	T_o (°K)	T_f (°K)
2	61	1.5	543	298	445
4	56	2.004	378	298	405
N-Michael	58	7.540	196	298	400

amounts of prodrug azacoumarin target **4** (i.e., up- or down-regulation was more pronounced). In our example of azacoumarin compound **4**, a full residual mass fraction for solving exact Arrhenius equation of the temperature will be 435 °K. The comparative data regarding both procedures are tabulated in Tables 2 and 3 that are outlined the products in good-to-excellent yields with simple and mild reaction conditions. The corresponding DGA that means the maximum equilibrium increase of a residual mass of the four samples in ratio (4:1, 3:1, 2:1 and 1:1 of the diethylmalonate/ethyl cyanoacetate) will be at 442 °K. If the temperature of DGA is greater than the half the TGA, it means more stability and fast transfer of producing a product (Figs. 3 and 4). Moreover, the temperature of minimum critical disorder of Gibbs entropy of the curcumin reactant **1** is 446 °K. The maximum temperature of conversion equilibrium of azacoumarins (**4** and **5**) and azachromone **6** is at 420 and 446 °K, which are closely confirmed with the temperature of Gibbs entropy (415 and 445 °K) referring to stop the reaction to afford azacoumarin **5** and azachromone **6** because any increase in temperature will make the reaction go in the opposite direction and give the high % yield of the azacoumarin **4** and unwanted N-Michael adduct (Figs. 5 and 6). Finally, the theoretical model can confirm us by the hard question when we can stop the reaction to afford azacoumarin **5** and azachromone **6** derivatives at ratio 4:1, 3:1 and 2:1 of the diethylmalonate/ethyl cyanoacetate, respectively (c.f. Schemes 1 and 2, and Figs. 7, 8, 9, 10 and 11).

To have a full residual mass fraction of azacoumarin compound **4** subsequently solving exact Arrhenius

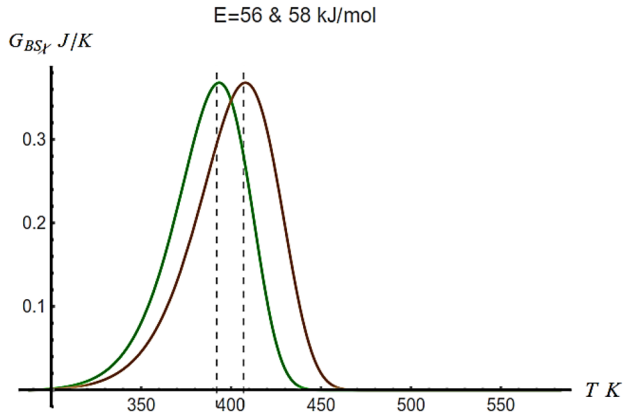

Fig. 10 $G_{SB\chi}$ of compounds 5 and 6 which capture the exact temperature (416 °K and 450 °K) of phase transition to new product at the lowest disorder of the chemical reaction

equation, the temperature will be 415 °K. The corresponding DGA that means the maximum equilibrium increase in a residual mass of the sample in ratio (1:1 of the diethylmalonate/ethyl cyanoacetate) will be at 422 °K. In addition, the temperature of minimum critical disorder of Gibbs entropy of the sample is 425 °K. The maximum temperature of conversion equilibrium of pyrid-2-one **2** and **3** is at 422 and 415 °K, which is confirmed with the temperature of Gibbs entropy (419 and 395 °K), respectively, which refers to stop the reaction of the pyrid-2-one **3**.

Results of DFT and Arrhenius model

We found from our study that quantum chemical calculation of DFT of Table 1 is approximately similar to the evaluated temperatures of exact solution of Arrhenius model as shown in Tables 2, 3, 4 and 5. The best alignment was obtained from the reaction with 2:1 and 1:1 ratios of the diethylmalonate/ethyl cyanoacetate, but the correlation was diminished when the reaction with the 4:1 and 3:1 ratios was evaluated. These results suggest that a stoichiometric ratio between reactant constituents and target prodrug azacoumarins **4**,

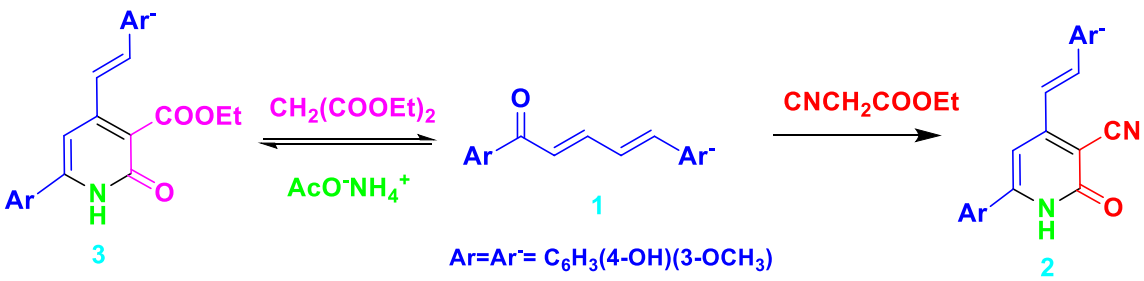

Scheme 2 It outlines the kinetic and thermodynamic control produce high yield of the product 2

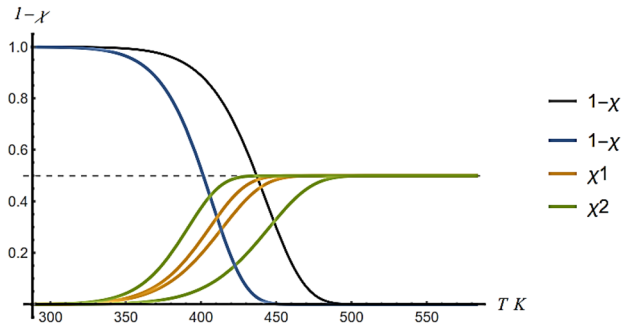

Fig. 11 TGA capture relation between chemical reaction of two reactants residual mass and their products of minimum full thermal mass decomposing temperature. The amount of absorb energy of azacoumarin product (**4**) is little high than azachromone product (**6**) than N-Michael adduct than azacoumarin product (**5**)

Table 4 The result of residual mass TGA, DGA, temperatures of conversion equilibrium point and its confirmation of finding Gibbs entropy using our exact model of Arrhenius equation the pyrid-2-one ester **3**, azacoumarin **5** and azachromone **6**

Compound	Maximum temperature of TGA	Maximum temperature of DTG	Maximum temperature of conversion equation	Gibbs entropy (J/K)	Time duration of full chemical process
3	415	422	–	425	127
$(1-\chi_i)$ 3	0.5	0.4	–	0.35	
5	–	417	422	419	
6	–	390	415	395	

Table 5 Activation energy and entropy of Arrhenius equation of the cyano pyrid-2-one ester **3**, azacoumarin **5** and azachromone **6**

Compound	Activation energy (KJ)	Exponential factor A $*10^6$	Entropy (J/mol)	T_0 (°K)	T_f (°K)
3	63	1.034	543	298	490
5	52	2.004	378	298	435
6	57	1.540	196	298	451

5 and azachromone **6** would be ideal for the generation of the reaction in which all reactant members exhibit affinity. However, different ratios are conceivable for the Arrhenius parameters (TGA, DTG, G_{SB}), which cover a wider range of electron affinities (A). In a situation where only a few good binders are present, their formation would more efficiently outcompete the others. Furthermore, in these types of organic compounds, all carbons are having sp^2 hybridization with hydrogen atom which produces the strongest type of covalent chemical bond. The electronegativity (χ) of carbon is 2.55 and hydrogen is 2.2. From these data, the difference between electronegativity of the atoms is 0.35. Thus, we may conclude that it is possible that the pyridine-2-one derivative **2** is attacked in the arylidene double-bond site by diethyl malonate even though soft–soft attack and the reaction mixture must have been acidic medium for promotion and afforded the 5,6-dihydro-anthranilic product **7**, i.e., it did not isolate in the normal condition (Scheme 3). So, the competitive energetically favorable prodrug azacoumarin **4** is formed while it has oxygen electronegativity of 3.44.

The oxygen atom has much more electronegative than either the hydrogen or the carbon, which are available in curcumin. Therefore, the O–H and O–C bonds in the hydroxyl group will be polar covalent bonds. The thermo-dynamical properties of excess parameters (TGA, DTG and G_{SB}) show that the nature of molecular interaction of prodrug curcumin **1**, 2-pyridinone **2** and azacoumarin **4** maybe suggests weak inter-molecular dispersive interaction between the mixing components (constituents) in certain range of concentration and strong interactions in certain other ranges. The percentage of deviation in velocity can be studied based on the interaction between the components of mixtures in equilibrium. It is predicted that the percentage of deviation in velocity shows either positive or negative deviations which are in equal numbers. This may be due to the molecular association and molecular dissociation of molecules which are taking part in all the systems. Normally, in the polar and nonpolar mixtures, there is a dipole-induced dipole interaction (μ), which is very weak in polar constituents. Azacoumarin is associative through hydrogen bonding, which mixes polar with nonpolar, resulting in the breaking of hydrogen

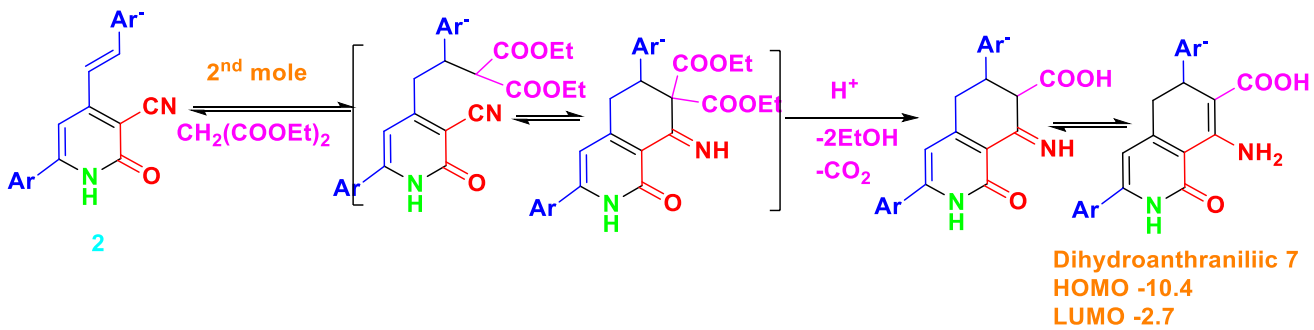

Scheme 3 It outlines the attack of the pyrid-2-one 2 and 3 at the arylidene active site by second molecule substituted ethyl acetate

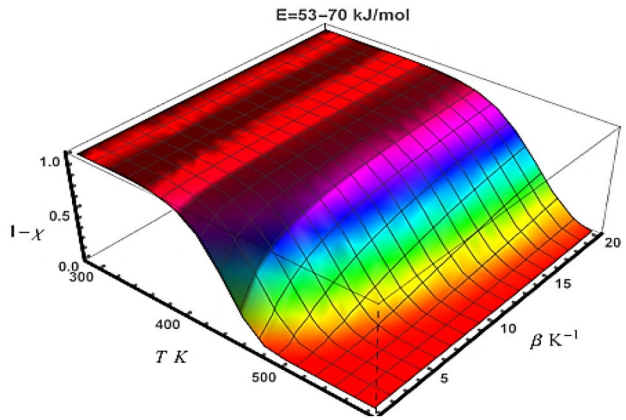

Fig. 12 The relation of azacoumarin product (**4**) between the residual mass, temperature and the increase in the rate of constant heat

bonding, thereby promoting dissociation [29, 30]. Though the magnitude of deviation also depends on concentration, the positive deviation observed is due to the molecular association and complex formation of molecules, whereas the negative deviations are due to the molecular dissociation of an associative molecule. Three-dimensional (3D) graph in Fig. 12 outlines the relation of azacoumarin product (**4**) between the reaction mixture of all residual mass and temperature with the increase in the rate of constant heat.

Conclusions

The ultrasonic velocities and densities for chalcone **1** and pyrid-2-one **2** afforded azacoumarin **4** which is more yielded than azacoumarin **5** and azachromone **6**. The results agree with the solution of the kinetic exact Arrhenius model and DFT simulation that shows the azacoumarin 4 is energetically more stable at temperature 422°K over the complete range of composition. By using the measurable physical properties such as hydration energy, ionization potential softness and hardness via DFT simulation based on quantum chemical computation as input parameters, these variables are inserted inside the exact kinetic model of Arrhenius solution to find that all values of kinetic stability of chemical reaction of temperatures have been estimated. The present work compared the experimental results of chemical stability of reaction at different temperatures with calculated simulated and theoretical parameters, and it finds that the mathematical Arrhenius kinetic model is in good agreement with experimental values.

References

1. P. Frei, L. Pang, M. Silbermann, D. Eriş, T. Mühlethaler, O. Schwardt, B. Ernst, Chem. Eur. J. **23**, 11570 (2017)
2. K.M. Swamy, W.B. Yeh, M.J. Lin, C.M. Sun, Curr. Med. Chem. **10**(22), 2403–2423 (2003)
3. J. Nielsen, Curr. Opin. Chem. Biol. **6**(3), 297–305 (2002)
4. A.T. Elgendy, A. AbdelAty, A. Youssef, M. Khder, K. Lotfy, S.J. Owyed, Math. Chem. (2019). https://doi.org/10.1007/s10910-019-01056-7
5. I.O. Zhuravel, S.M. Kovalenko, A.V. Ivachtchenko, K.V. Balakin, V.V. Kazmirchuk, Bioorg. Med. Chem. Lett. **15**, 5483–5487 (2005)
6. C. Calliste, J.L. Bail, P. Trouillas, C. Pouget, G. Habrioux, A. Chulia, J. Duroux, Anticancer Res. **21**, 3949–3956 (2001)
7. Z.-G. Yang, H.-X. Sun, W.-H. Fang, Vaccine **23**(44), 5196–5203 (2005)
8. G. An, C. Seifert, G. Li, Org. Biomol. Chem. **13**, 1600–1617 (2015)
9. J. Trilleras, P. De La Torre, D.J. Pacheco, J. Quiroga, M. Nogueras, J. Cobo, Lett. Org. Chem. **8**, 652–655 (2011)
10. I. Gülçin, M. Oktay, O. Küfrevioglu, J. Ethnol. Pharmacol. **79**(3), 325–329 (2002)
11. A. Elkholy, S.A. Rizk, A. Rashad, J. Mol. Struct. **1175**, 788–796 (2019)
12. S. Rizk, A. El-Naggar, A. El-Badawy, J. Mol. Struct. **1155**, 720–733 (2018)
13. D. Wang, Y. Wang, J. Zhao, M. Shen, J. Hu, Z. Liu, L. Li, F. Xue, P. Yu, Org. Lett. **19**(5), 984–987 (2017)
14. T. Narumi, H. Takano, N. Ohashi, A. Suzuki, T. Furuta, H. Tamamura, Org. Lett. **16**(4), 1184–1187 (2014)
15. H.Narumi Takano, T. Nomura, H.W. Tamamura, J. Org. Chem. **82**(5), 2739–2744 (2017)
16. S.A. Rizk, M.A. El-Hashash, A. El-Badawy, J. Het. Chem. **54**, 2003–2011 (2017)
17. S.A. Rizk, G.A. El-Sayed, M.A. El-Hashash, J. Iranian Chem. Soc. **15**, 2093–2105 (2018)
18. S.A. Rizk, S. Shaban, H.A. Sallam, J. Het. Chem. (2019). https://doi.org/10.1002/jhet.3833
19. E. Eser, H. Koç, J. Sci Tech **9**(1), 27–31 (2019)
20. V. Aquilanti, N.D. Coutinho, V.H. Carvalho-Silva, Philos. Trans. R. Soc. A **375**, 20160201 (2017). https://doi.org/10.1098/rsta.2016.0201
21. S. Goldstein, D.A. Huse, J. L. Lebowitz, P. Sartori, (2017a). http://arxiv.org/abs/1712.08961
22. D. Lazarovici, (2018). http://arxiv.org/abs/1809.04643 48
23. S. Ladame, Org. Biomol. Chem. **6**, 219–226 (2008)
24. M. Hamidi, H. Tajerzadeh, Drug Deliv. **10**(1), 9–20 (2003)
25. A.F. Fahmy, S. Rizk, M. Hemdan, A. El-Sayed, I.J. Hasaballa, Het. Chem. **55**, 2545–2554 (2018)
26. S.A. Abdel-Latef, A.S. Darwish, S.A. Rizk, S.K. Atya, M.E. Helal, J. Mol. Liq. **288**, 111006 (2019)
27. S.K. Attia, A.T. Elgendy, S.A. Rizk, J. Mol. Struct. **1184**, 583–592 (2019)
28. S.A. Rizk, G. Elsayed, M.A.J. El-Hashash, Iranian Chem. Soc. **15**, 2093–2105 (2018)
29. F. Aparicio, M.J. Mayoral, C. Montoro-Garci, D. Gonza´lez-Rodrı´guez, Chem. Commun. **55**, 7277–7299 (2019)
30. M.C. Stumpe, H. Grubmüller, J. Am. Chem. Soc. **129**, 16126–16131 (2007)